H_2-D_2, and HD-D_2 the thermal conductivity of any mixture of the three gases can be calculated by means of the numerical relations below in which the chemical symbols represent the mole fraction of each gas in the mixture.

$$K_M \times 10^5 = \left[41.8\left(\frac{H_2}{H_2 + HD}\right)^{1.0338} + 34.12\left(\frac{HD}{H_2 + HD}\right)^{1.0414}\right]\left(\frac{H_2 + HD}{2}\right) + \left[41.8\left(\frac{H_2}{H_2 + D_2}\right)^{1.0338} + 29.56\left(\frac{D_2}{H_2 + D_2}\right)^{1.0478}\right]\left(\frac{H_2 + D_2}{2}\right) + \left[34.12\left(\frac{HD}{HD + D_2}\right)^{1.0414} + 29.56\left(\frac{D_2}{HD + D_2}\right)^{1.0478}\right]\left(\frac{HD + D_2}{2}\right) \quad (17)$$

APPLICATION TO EQUILIBRATED MIXTURES

If 4.00 is taken as the value of the equilibrium constant in Equation 1 the composition of the equilibrated mixture resulting from a binary mixture containing 1 mole of hydrogen and x moles of deuterium is given by the relations

Gas	Moles	Mole fraction
HD	$2x/(1 + x)$	$2x/(1 + x)^2$
H_2	$1/(1 + x)$	$1/(1 + x)^2$
D_2	$x^2/(1 + x)$	$x^2/(1 + x)^2$

(18)

Table II contains the composition of the hydrogen-deuterium mixtures and their observed thermal conductivities as plotted in Figure 2. Table II also contains the composition of the ternary mixtures as calculated by the Relations 18. Finally the experimental thermal conductivities of the equilibrated mixtures are compared with those calculated from the curve for E = 4.00 in Figure 3.

LITERATURE CITED

(1) Archer, C. T., *Proc. Roy. Soc.* (*London*) **A165,** 478 (1938).
(2) Bolland, J. L. Melville, H. W., *Trans. Faraday Soc.* **33,** 1316 (1937).
(3) Buddenberg, J. W., Wilke, C. R., *Ind. Eng. Chem.* **41,** 1345 (1949).
(4) Farkas, A., Farkas, L., *Proc. Roy. Soc.* (*London*) **A144,** 467 (1934).
(5) Ibbs, T. L., Hirst, A. A., *Ibid.*, **A123,** 134 (1929).
(6) Lindsay, A. L., Bromley, L. A., *Ind. Eng. Chem.* **42,** 1508 (1950).
(7) Van Cleave, A. B., Maas, O., *Can. J. Research* **12,** 57 (1935).
(8) *Ibid.*, p. 372.
(9) Wassiljewa A., *Physik Z.* **7,** 235 (1904).

RECEIVED for review July 7, 1958. Accepted December 11, 1958.

Effect of Molecular Structure on Burning Velocity

G. J. GIBBS and H. F. CALCOTE[1]
Experiment Inc., Richmond 2, Va.

The burning velocities of various compounds have been investigated by many observers in an attempt to understand the mechanism of flame propagation. These data have been obtained by four general methods: the propagation of flame in a tube, in a spherical bomb, in a soap bubble, and on a Bunsen burner (*3, 4, 8, 12, 16, 17, 22, 23, 30, 36*). Such data on many fuel types are important in verifying theories of flame propagation and ignition and the data reported herein have already been so employed (*11, 24, 32*). By altering the fuel structure (*6*), the data are made available for examining such considerations and for predicting the burning velocity of most new systems. Combustibles for which good burning-velocity data are already available have also been studied, to demonstrate the degree to which such data, taken in different laboratories and by different methods, can be compared.

To carry out this program successfully, it is necessary to have a simple yet reliable method of calculating the burning velocity from the flame dimensions. Although there are a number of methods for determining burning velocities from Bunsen burner flame cones, those which have a reasonable theoretical basis and give reliable results require somewhat detailed measurements or calculations (*14, 15, 19, 31, 33, 34*). This report presents a simple procedure which requires a minimum of calculations to obtain reliable results with data demonstrating the errors involved, a comparison with results from other laboratories, and the burning velocities of 77 compounds showing the effect of molecular structure on burning velocity.

APPARATUS AND PROCEDURE

The apparatus is basically the same as that used by other investigators. Provision is made for controlling and measuring flow rates of air, gaseous fuels, and liquid fuels. The liquid fuels are vaporized and fed to the burner in the gaseous form (*5*). Air is taken from the laboratory supply and metered with a sonic-orifice flowmeter. Gaseous fuels are taken directly from tanks and the pressure is controlled with a Moore Products Nullmatic pressure regulator; the flow rate is determined with a sonic-orifice flowmeter calibrated for each gas. A mixing chamber containing two porous stainless steel disks and filled with glass Raschig rings both aids mixing and prevents flashback through the gas-feed tubes. All tubing and valves with which the gas comes in contact beyond the liquid-fuel-injection system are Type 316 stainless steel. The burners are seamless stainless steel tubing which can be easily exchanged at a flange on the mixing chamber. Both the air meter and gaseous fuel meter are calibrated by a water-displacement method.

The flame is photographed with a Speed Graphic camera having an f 4.7 lens using Ansco SSS-Ortho film, varying exposure times from 1/25 to 1/100 second. Shadowgraphs of the flame are made by photographing the shadow formed by the heated gases in the inner cone refracting the light from a 2-watt Western Union concentrated arc lamp serving as a point of light source. A Speed Graphic camera without a lens is used, and the exposure time (1/15 to 1/25 second) is controlled by a focal-plane shutter. The burner is placed between the lamp and the film, 61 cm. from the lamp and normally 30 cm. from the film. A scale is photographed on each picture for determining the magnification factor, M.

The methodology involved in calculating burning velocities from the photographs or tracings was derived by considering the volume rate of flow through a section of the flame surface over which the burning velocity is essentially constant. This condition is satisfied if the tip and base of the flame are neglected. Then, the burning velocity is equal to the volume rate of gas flow through a lateral area of the frustum of flame surface divided by that lateral area. The volume rate of gas flow

[1] Present address, AeroChem Research Laboratories, Inc., P. O. Box 12, Princeton, N. J.

through such a frustum is obtained by integrating the linear flow velocity between the radii which define the annular flow entering the frustum of cone considered. This assumes that a flow stream does not change its direction after leaving the burner port until it enters the combustion region. The burning velocity, S_u is, in terms of the total volume flow rate, V, and the slant height of the frustum, h:

$$S_u = (V/h)k \tag{1}$$

where, in terms of frustum diameters, d:

$$k = \frac{C_1(d^2_2 - d^2_1) - C_2(d^4_2 - d^4_1)}{d_2 + d_1} \tag{2}$$

C_1 and C_2 are constants for a given burner diameter, D:

$$C_1 = 4/\pi D^2 \quad - C_2 = 2/\pi D^4 \tag{3}$$

Since the apex of a shadowgraph is sharp (Figure 1), simplification is possible by considering the cone from the point where the sides begin to curve to the apex (d_1 then becomes equal to 0), and Equation 2, for k, becomes

$$k = \frac{C_1 d^2_2 - C_2 d^4_2}{d^2} \tag{4}$$

The calculations have been further simplified for a given burner by setting up tables of k values for all necessary values of d_2. Then, to calculate the burning velocities, one needs only to place V, k, and h in Equation 1.

The diameter and the slant height are measured from photographic enlargements and the actual sizes obtained from the magnification factor, M. When a cone is taken from shadowgraphs, the negatives are projected in an enlarger on a sheet of paper where lines are drawn parallel to the sides. Measurements are made from this tracing without the necessity of making a print. The burning velocities are plotted as a function of the equivalence ratio, ϕ, the stoichiometric air-fuel ratio divided by the actual air-fuel ratio. This method of determining burning velocities will be referred to as the "apex-cone" method.

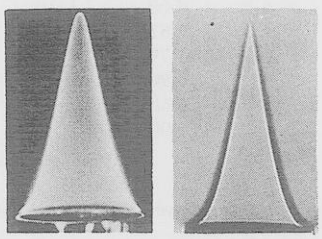

Figure 1. Luminous cone and shadowgraph of Bunsen burner flame
n-Pentane–air flame at 25° C.; Burning velocity, 42 cm./sec.; Volumetric flow rate, 124 cc./sec.; Burner diameter, 1.10 cm.; ϕ = 1.00

VALIDITY OF EXPERIMENTAL TECHNIQUES

Before measuring the burning velocity of a series of fuels, one must examine both the possible factors which may cause errors and the ability to check results obtained in other laboratories.

For any method to be of value, the burning velocity should be independent of burner diameter, total laminar-flow velocity, and what one chooses as the flame surface, because all of the flame must be propagating at the same velocity relative to the unburned gas mixture. Thus burning velocities should be the same when measured on shadowgraphs or luminous cones if proper considerations are made.

Burner Diameter. The effect of burner diameter is demonstrated in Figure 2 for four different burner diameters between 0.452 and 1.737 cm., a ratio of diameters of 3.8 to 1. No change in burning velocity is observed over this range. At least two different burner diameters have always been employed to assure that for the particular fuel the burner diameter had no effect.

Total Flow Rate. The effect of total flow rate on the burning velocity is demonstrated in Table 1. The only appreciable deviation occurs at the very low flow rate of 31 cc. per second, where the flame is extremely small. Doubling the flow rate, 62 to 122 cc. per second, gave no deviation beyond the experimental error. Since all of the flame cones outside of this range (on the size of burners employed) are either so tall or so short as to be obviously poor subjects for study, there is little chance for error due to flow velocity. The data were taken over a period of several days, hence show the reproducibility to be expected.

Film to Flame Distance. Other observers (*1, 2, 21*) agree that the outer edge of the shadow cone—i.e., the outer edge of the light area on the shadow negative—is a true image of the reaction zone and that extrapolation to zero distance between the photographic plate and the flame shows that the outer cone and the sharp inner cone coincide, and that the outer cone is the proper place to make burning-velocity measurements because this image is not affected by refraction of the light as is the cone defined by the inner black-white edge. The real objection to using the outer cone, however, lies in the inability to make accurate, reproducible measurements because of the lack of sharpness. At a film-flame distance of 30 cm., using the apex-cone method on the inner and outer cones of randomly selected flame shadowgraphs with varying fuels and fuel-air ratios, burning-velocity values are obtained which compare favorably. Sixty-nine different shadowgraphs of 14 fuels and fuel mixtures at various air-fuel ratios and initial temperatures were compared.

Effects on Burning Velocity

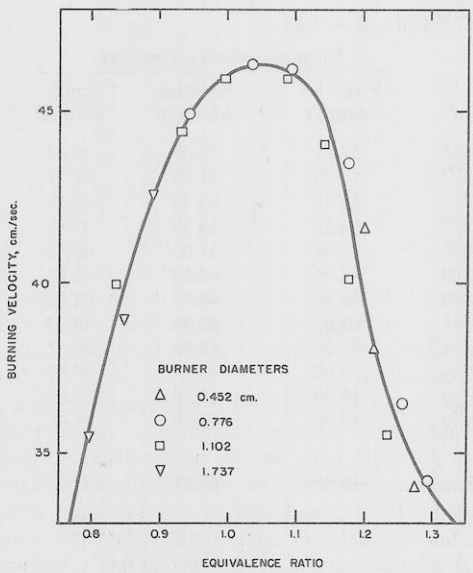

Figure 2. Shadowgraphs of propane-air flames (apex-cone method)

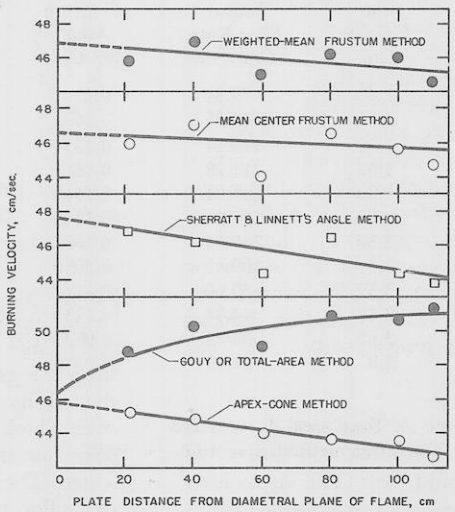

Figure 3. Ethane-air at ϕ = 1.02; Total flow, 88 cm./sec.; Burner diameter, 1.10 cm.

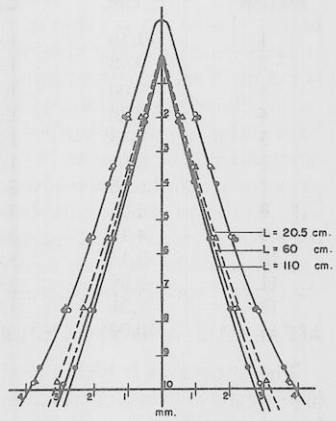

Figure 4. Tracings of ethane-air flames (ϕ = 1.02) at film to flame distances, L

Table I. Effect of Total Flow Rate on the Burning Velocity of Propane-Air Flames

(Apex-cone method)
Burner diam: 0.766 cm.

Equivalence Ratio ϕ	Flow Rate, Cc./Sec.	Burning Velocity, Cm./Sec. Measured	Mean	% Dev. from Mean	Av. % Dev. from Mean
0.922	31.0	(49.98)[a]		(+ 17.57)	
	31.0	(44.87)		(+ 5.55)	
	62.3	41.36		- 2.71	
	62.3	41.51		- 2.35	
	83.0	43.21		+ 1.65	
	83.0	43.98	42.51	+ 3.46	2.54
0.997	31.0	(51.59)		(+ 12.74)	
	62.3	45.60		- 0.35	
	62.3	46.18		+ 0.92	
	83.0	46.68		+ 2.01	
	122.0	44.58	45.76	- 2.58	1.46
1.18	62.3	43.09		- 3.83	
	62.3	44.53		- 0.47	
	122.0	44.57		- 0.38	
	122.0	45.28		+ 1.21	
	122.0	46.21	44.74	+ 3.29	1.84
				Av. error[b] =	2.08%

[a] Figures in parentheses not included in determining the averages.
[b] Includes experiments not recorded in table.

The average deviation of the outer cone value from the inner cone value was only 3.95%. The average deviation when the outer cone value exceeded the inner cone value was 5.87%, and when it was less, 2.04%.

The burning velocity reported herein, decreased with increasing film to flame distance, while others (*1*, *21*) found an increase with distance. This led to a closer examination of the results. Figure 3 shows the data obtained by analyzing a series of shadowgraphs by different methods, all employing the inner black-white edge. In the top curve the burning velocity at each point was obtained by a weighted average according to surface areas for seven to nine frustums excluding the bases. In the second curve the burning velocities from four to five frustums, excluding the tips and bases, were averaged. The next curve was obtained by using the angle method of Sherratt and Linnett (*31*), which gives results in the opposite direction from those reported by Grove, Hoare, and Linnett (*21*). There are insufficient data in the latter article to explain this difference. The results from the total-area and apex-cone methods are also reported. When the outer black boundary was used, the burning velocity did not vary with film-flame distance; then the burning velocity was 46.2 cm. per second. The burning velocity at ϕ = 1.02 from the curve of burning velocity *vs.* equivalence ratio obtained by the standard procedure was 45.2 cm. per second.

The results of Figure 3 are easily understood by reference to Figure 4. The shadowgraphic tracings of the same ethane-air flame are presented at three different film-flame distances. The inner three lines are for the black-white boundary. The outer line is for the outer black boundary. Inspection will show that any method based upon the outer black boundary will give results independent of film-flame distance as pointed out by Grove, Hoare, and Linnett. Results based upon the black-white boundary (inner three lines) will depend upon the method of analysis. Any method based upon the angle the flame surface makes with a flow line should give a decrease in burning velocity with increasing distance. Any frustum method should

Table II. Calculation of Burning Velocities by the Frustum and Total-Area Method

(Luminous cone, butane-air mixture)
Magnification, 10.5. Flow rate, 85.8 cc./sec.
Burner diameter, 0.766 cm. ϕ = 1.05

Cone Section[a]	Diameter, d_i, Cm.	Slant Height, Cm.	Area, A, Sq. Cm.	Burning Velocity, S, Cm./Sec.	$S \times A$
1	8.80	1.11	0.2435	17.38	4.233
2	7.60	1.00	0.2120	28.01	5.937
3	6.88	1.68	0.308	36.06	11.107
4	5.99	1.68	0.2638	38.44	10.138
5	5.30	3.80	0.5035	41.06	20.672
6	4.00	3.80	0.3687	46.03	16.971
7	2.81	3.21	0.2104	52.07	10.956
8	1.79	2.60	0.0997	59.32	5.913
9	0.90	0.50	0.0113	78.15	0.880
10	0.68	0.40	0.0039	302.4	1.170
	0.00				
		Total area =	2.225		87.977

Area weighted average of burning velocity = $\frac{87.98}{2.225}$ = 39.54 cm./sec.

[a] From base of cone to apex.

Table III. Comparison of Methods of Calculating Burning Velocities

(Shadowgraph, butane-air flame)
Magnification, 15.67 Flow rate, 85.8 Cc./Sec. Burner diameter, 0.776 Cm. ϕ = 1.05

Cone Section[a]	Diameter, d_i, Cm.	Vertical Height, Cm.	Slant Height, Cm.	Linear Flow Rate, Cm./Sec.	Frustum Area,[a] Sq. Cm.	Sin α[b]	Burning Velocity, Cm./Sec. S and L's Method[c]	Frustum Method	Angle Method
1	11.50	1.41	1.60	79.84	0.2194	0.3838	37.85	38.04	30.64
2	9.98	1.30	1.35	141.89	0.1637	0.3507	49.96	51.86	49.76
3	9.00	1.11	1.20	179.64	0.1334	0.2703	55.45	53.38	48.56
4	8.28	1.58	1.60	211.28	0.1605	0.2507	55.55	55.59	52.97
5	7.43	1.80	1.80	241.91	0.1618	0.2007	53.68	54.00	48.55
6	6.61	1.71	1.80	265.21	0.1455	0.1729	47.45	44.44	45.86
7	6.00	2.31	2.30	285.64	0.1652	0.1590	48.84	48.91	45.42
8	5.21	3.45	3.49	309.63	0.2081	0.1561	48.83	47.93	48.33
9	4.11	3.30	3.39	330.60	0.1571	0.1534	47.57	45.83	50.71
10	3.15	3.61	3.68	344.94	0.1233	0.1420	50.02	49.27	48.98
11	2.09	3.45	3.48	356.22	0.0732	0.1420	44.96	44.44	50.58
12	1.21	4.75	4.8	361.99	0.0370	0.1420	46.05	44.85	51.40
	0.00								
			Total area, A_T =	1.748		$S_{av.}$ =	48.85	48.21	47.65
			Total area method, $S = V/A_T$ =	49.07					

[a] From base of cone to apex.
[b] Sin α measured by drawing a tangent to curve for angle method.
[c] Sherratt and Linnett, (*31*).

give a decrease in burning velocity with increasing distance because the area of the frustum increases with distance. This is shown by drawing vertical lines for flow lines (Figure 4) which define the frustum diameters; the slant height increases with increasing distance. The frustum method on the outer black edge and the black-white boundary will give the same result when these two edges are parallel; the outer cone is simply considered to be displaced downstream. Because the total area of the three inner tracings decreases with increasing distance, the burning velocity should increase for any total-area method which utilizes the shadowgraph technique. Compare the areas 2.225 sq. cm. with 1.748 sq. cm. (Tables II and III) for evidence that the total surface area is less for the shadowgraph than for the luminous cone. The total-area method assumes that the apparent increase in burning velocity at the apex of the luminous cone and the decrease in burning velocity near the base cancel each other, which is not the case. The area at the base with low burning velocity is considerably larger than the area at the apex where burning velocity is high (Table II). There is no appreciable change in burning velocity near the apex of a shadowgraph (Table III), although the burning velocity is reduced near the base. The frustum method also gives a low value for luminous cones when a large number of frustums are averaged.

Methods of Data Analysis. Four different methods of analyzing a single cone have been applied to the data in Table III. The agreement among the methods is rather good. However, Table IV demonstrates that by considering only a large top frustum, actually a cone of a shadowgraph, values may be obtained which are comparable with those obtained by any of the acceptable methods either on shadowgraphs or luminous cones. Analysis of randomly selected shadowgraphs for seven completely different fuels at various initial temperatures and air-fuel ratios corroborated this statement. Therefore, it is possible to obtain reliable results by the apex-cone method.

Propane-Air Flames and Effect of Water. The results for propane-air flames measured by different methods in different laboratories are summarized in Figure 5. Those obtained in this work contained normal laboratory air (0.31 mole % of water in air) at 25° C. and air saturated with water (3.1 mole % of water in air). The data were obtained on various sizes of thermally jacketed burner tubes at widely varying flow rates using the apex-cone method and shadowgraph technique. Results were checked in a closed system and in open room air. The curves of Singer (*33*) were obtained on a cylindrical and a slot burner tube using air dried over calcium chloride and calculations made using Dery's truncated-cone method described in reference (*25*). The slot-burner data agreed with results obtained in a spherical bomb (*28*). The curve of Andersen and Fein is a composite of two curves (*1*), the lean side of which was obtained using the total-area method on shadowgraphs, extrapolated to zero film-flame distance, and the rich side obtained using stroboscopically illuminated particle tracks. They used a Mache-Hebra nozzle at 25° C. with less than 0.07 mole % of water in the fuel-air mixture.

Gray, Linnett, and Mellish (*20*) have compared the burning velocities of propane-air mixtures obtained by eleven different observers. Figure 3 of their article illustrates the variety of data which exists on burning velocity. The highest maximum burning velocity shown in that curve is 1.5 times as great as the lowest maximum value. Linnett and associates have discussed the various methods of determining burning velocities, the reasons for data being high and low, etc., but they do not mention the effects of initial mixture temperature and moisture in the gaseous mixture. Unfortunately, many observers fail to record these two very important parameters. Before a useful value for the burning velocity of any fuel can be declared, the initial temperature, pressure, moisture content, and fuel composition must be stated. Gray, Linnett and Mellish (*20*), "after considering the various methods," decided that their curve and that of Andersen and Fein (Figure 5, this article) "are obtained by methods least likely to lead to serious error." They

Table IV. Burning Velocity of *N*-Butane-Air Flames by Different Methods

	A. Shadowgraph		B. Luminous Cone			
	ϕ = 1.05		ϕ = 1.16		ϕ = 1.29	
Method	A	B	A	B	A	B
Frustum, av. of 3	46.9	47.9	42.4	44.1	37.5	35.0
Frustum, top only or apex cone	47.0	...	42.8	...	35.4	...
Frustum, weighted height	47.4	49.8	47.3	45.6	39.7	39.3
Method of Sherratt and Linnett[a]	47.6	...	...	...	...	...
Angle method	47.6	...	...	...	...	...
Frustum, av.	48.2	...	49.0	...	41.6	...
Frustum, weighted area	48.2	39.5	49.1	38.7	41.3	33.1
Total area, $S = V/A_T$	49.1	38.6	48.4	37.7	42.4	33.2

[a] Averaged from cone sections 6 to 12 in Table III.

suggest that the "maximum burning velocity for propane-air mixture is 44 ● 1 cm. per second when the percentage of propane present is 4.3 ± 0.15" (ϕ = 1.02). This value was apparently determined from an average of the maximum values of the selected curves, that of Andersen and Fein being obtained at 25° C. with 0.07 mole % of water in the fuel-air mixture and Gray's being obtained at 11° C. with the moisture content not reported. The data given in Table 3 of Gray's article (*20*) for the schlieren "slit" procedure at 11° C. and 1.0 atm. coincide with the authors' data which were obtained with 3.1 mole % of water in air at 25° C. and 1.0 atm. If Gray's fuel-air mixture was relatively dry, a correction for initial temperature would raise their curve to coincide with the authors' 0.31 mole % of water in air curve.

Ethylene-Air Flames and Effect of Water. Further comparison with Linnett and his associates is illustrated in Figure 6 for ethylene-air. Three methods were employed by Linnett to obtain the data shown. Pickering and Linnett (*29*) used a modified angle method on shadowgraphs which neglected the burning velocity near the apex and base of the cone. These values were taken from the article of Linnett and Hoare (*26*) (which were corrected by extrapolation to zero film-flame distance). The other values are those obtained by Conan and Linnett (*9*) using the angle method on schlieren photographs and those of Linnett, Pickering and Wheatley (*27*) using schlieren photography and the soap-bubble technique. Strehlow and Stuart (*35*), employing a soap-bubble technique, recorded data agreeing with those of Linnett and associates. The three methods are compared with the two ethylene-air curves obtained by the authors with 0.31 and 3.1 mole % of water in air. Linnett and Hoare have stated their initial temperature to be 16° ± 2° C., but Conan and Linnett (*9*) and Pickering and Linnett (*29*) did not specify the initial temperature. No reference was made in either case to the moisture content of the gaseous mixture. Linnett and Hoare (*26*) have studied flame propagation along horizontal tubes, reporting a maximum burning velocity of 69.7 cm. per second at ϕ = 1.05 (6.87 volume % of ethylene). The maximum burning velocity is in agreement with the values obtained using the burner-tube and soap-bubble methods; however, the concentration of ethylene at the maximum is lower. They were unable to offer any explanation for this difference but have pointed out that the maximum in the curve of burning velocity *vs.* composition for propylene-air flames was at the same percentage for both tube (*18*) and burner methods (*20*); however, for propane-air flames all burner methods (*20*) gave the maximum burning velocity at the same percentage, but the maximum in the curve obtained by the tube method (*18*) was at a higher percentage. The data from the Bureau of Mines were obtained on a slot burner and agreed with spherical-bomb results. Dugger (*10*) reports a maximum burning velocity for ethylene of 64.0 cm. per second (ϕ = 1.16) at 25° C. using the Bunsen burner technique.

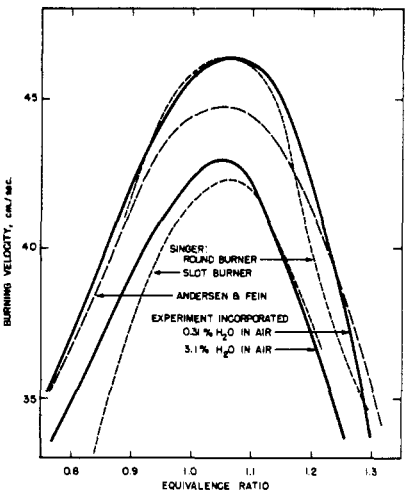

Figure 5. Propane-air flames, 25° C.

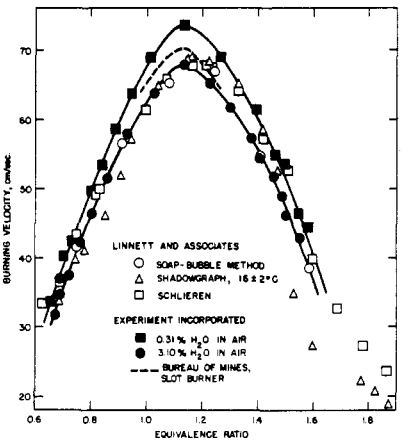

Figure 6. Ethylene-air flames, 25° C.

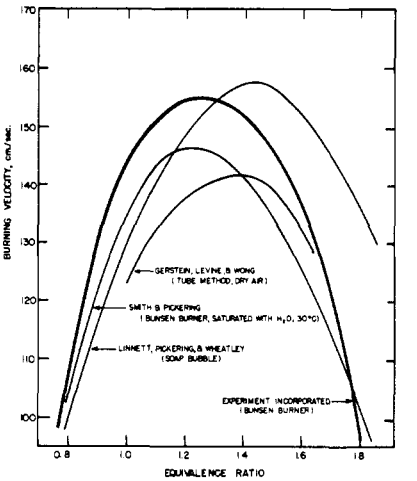

Figure 7. Acetylene-air flames

Burning Velocities

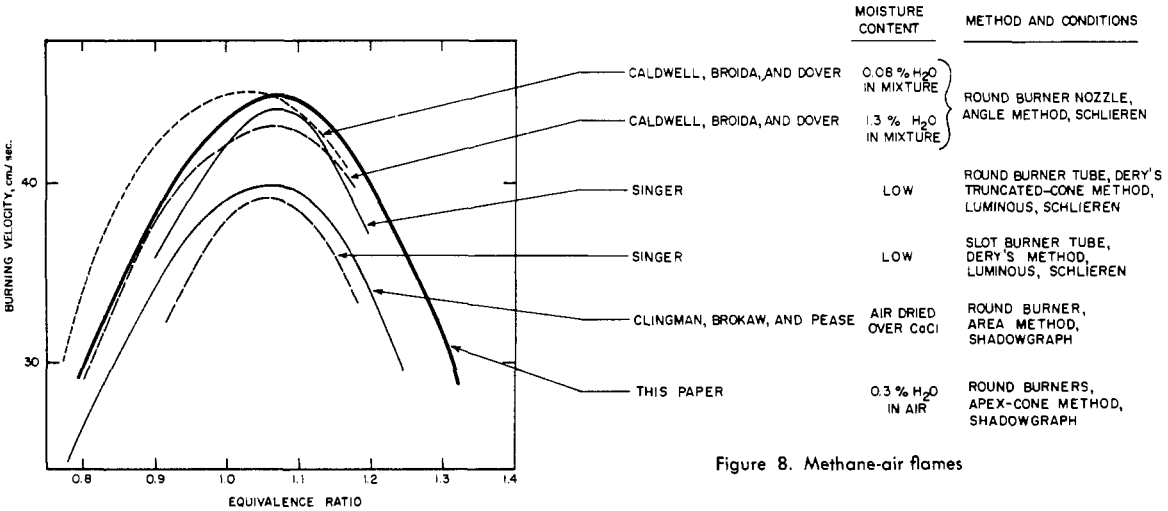

Figure 8. Methane-air flames

Acetylene-Air. A comparison of the Bunsen burner, the flame-tube, and the soap-bubble methods is offered in Figure 7. The agreement for burning velocities is not too unsatisfactory considering the difference in conditions. However, the different equivalence ratios at which the maximum burning velocity occurs is somewhat surprising. The Bunsen burner methods give maxima at the same composition, while the soap-bubble and tube methods agree with respect to the composition for maximum burning velocity. This difference might be due to the methods, except that Friedman and Burke (*13*) employing the tube method found the maximum flame velocity at $\phi = 1.25$ in agreement with the authors' value.

Methane-Air. Another comparison is made in Figure 8; this time for methane-air flames. The most outstanding feature of this comparison is that the maximum burning velocity occurs at approximately the same equivalence ratio, whereas for most other fuels different observers obtain widely scattered maxima. Caldwell, Broida, and Dover (*7*) have obtained a slight increase in equivalence ratio at which the burning velocity is a maximum by the addition of water vapor. The burning velocity decreased. The two curves shown in Figure 8, which were obtained by Singer (*33*), illustrate the effect of using slot burners as compared with round burners. The truncated-cone method of Dery (*25*) was employed in both cases at 25° C. and 1.0 atm. The curve of this article was obtained as explained for other fuels.

Comparison with Flame Propagation in a Tube. The present burning velocity data obtained by the Bunsen burner method and the flame speed of flame propagating in a tube are compared with those of Gerstein, Levine, and Wong at NACA (*18*) in Figure 9, where volume per cent fuel at maximum flame velocity from NACA (*18*) is plotted against that obtained in this laboratory. If this line were extended to 10%, methane would fall on the curve and acetylene above it. The relationship is linear, the maximum burning velocity occurring slightly on the rich side for the tube data. Figure 10 is a correlation at maximum burning velocities as obtained by the two laboratories; the tube method gives lower values.

Singer (*33*) has recently compared burning velocities determined on cylindrical and slot burners and in a spherical bomb. He has demonstrated by analysis and comparison of Bunsen flames from both cylindrical and slot burners that lower burning velocity results when the latter method is used, owing to removal of the effect of curvature of combustion surface as predicted by theory (*25*). Furthermore, he has found agreement between the slot-burner method and the spherical-bomb method which is within experimental error. Preliminary studies on slot burners using a propane-air flame at Experiment Inc. are in very close agreement with the results reported by Singer.

Although questions still remain about correct methods for obtaining "absolute" values of burning velocities, the method employed in this report is useful in determining effects due to changes in molecular structure.

RESULTS AND DISCUSSION

The results are summarized in Tables V and VI for a range of equivalence ratios at initial temperatures of 25° and 100° C. These data have been taken from an averaged curve through experimental points with an accuracy as indicated in the previous section. In each experiment the equivalence ratio increments were less than 0.1 unit. The averaged curves are presented in Figures 11 through 25 for the 25° C. data and Figures 26 through 32 for the 100° C. data. Fuels are grouped according to molecular structure for purposes of comparison.

(*Text continued on page 235*)

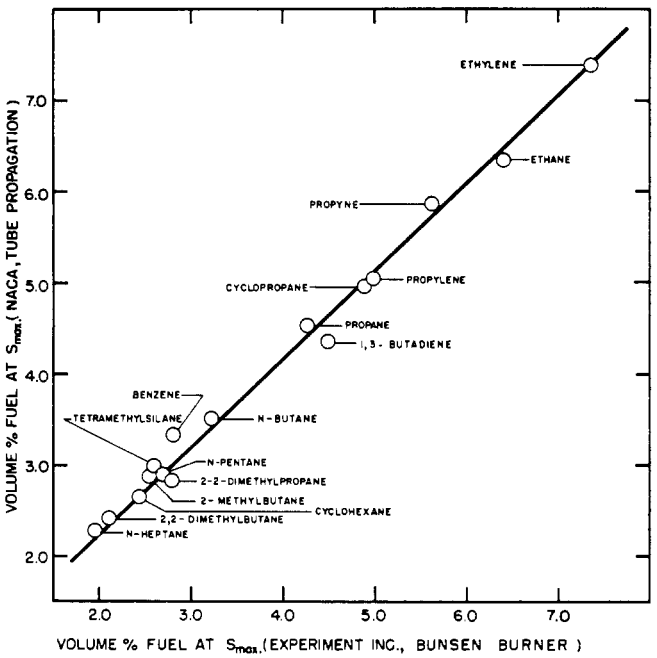

Figure 9. Compositions at which maximum burning velocity occurs on a Bunsen burner and in a tube

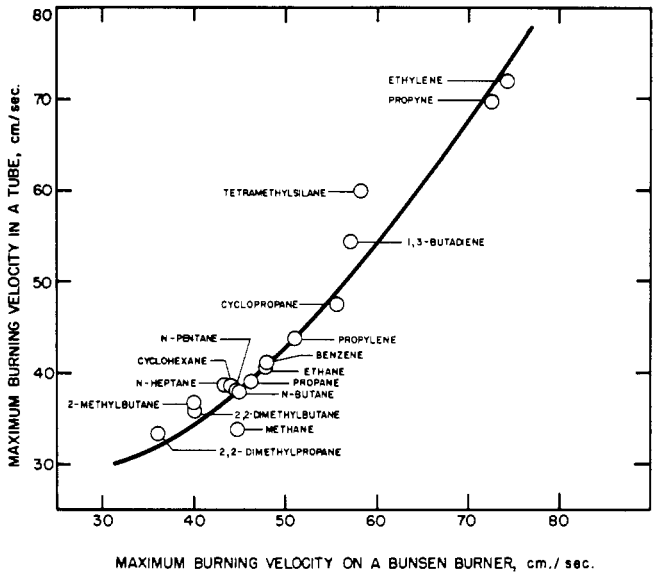

Figure 10. Maximum burning velocities obtained on a Bunsen burner and in a tube

Burning Rates at 25° C.

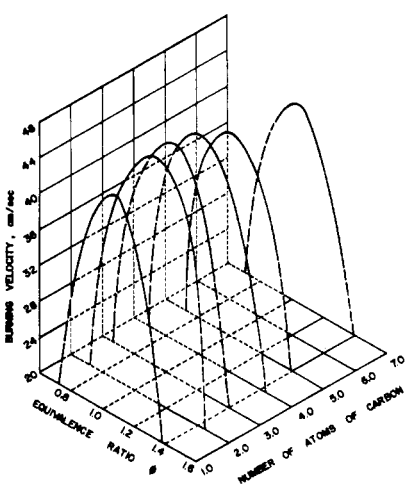

Figure 11. Normal alkane hydrocarbons

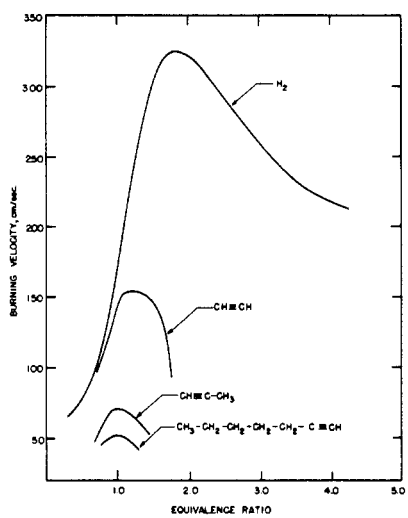

Figure 12. Acetylenes and hydrogen

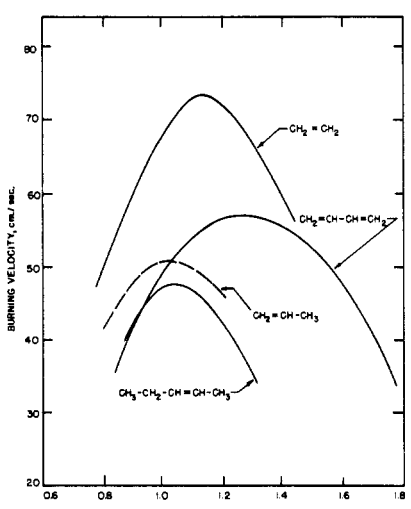

Figure 13. Ethylenes

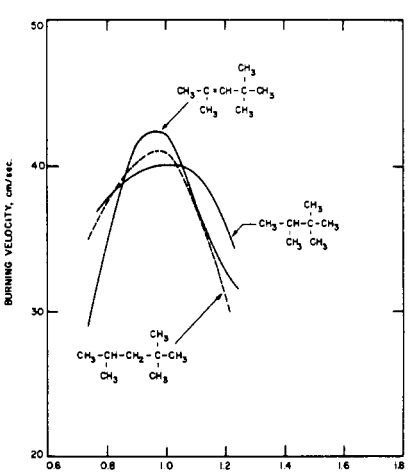

Figure 14. Branched hydrocarbons

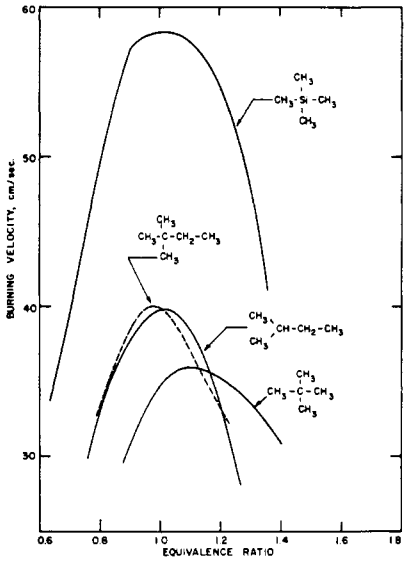

Figure 15. Branched hydrocarbons and tetramethylsilane

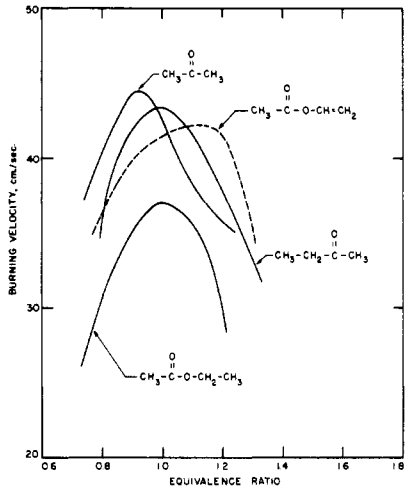

Figure 16. Secondary substituted hydrocarbons

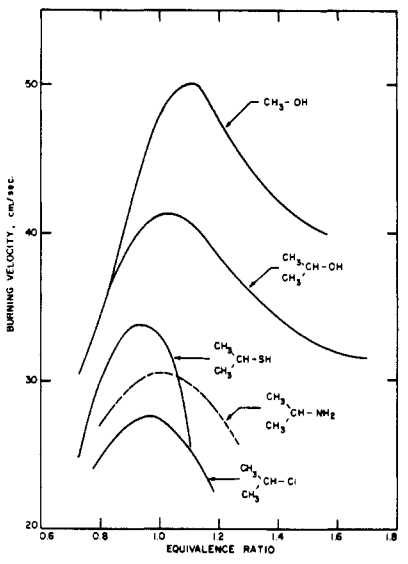

Figure 17. Secondary substituted hydrocarbons

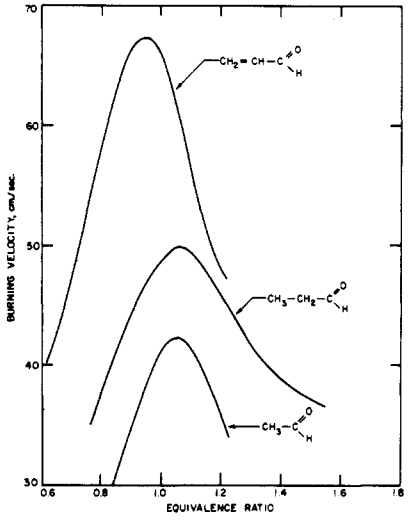

Figure 18. Aldehydes

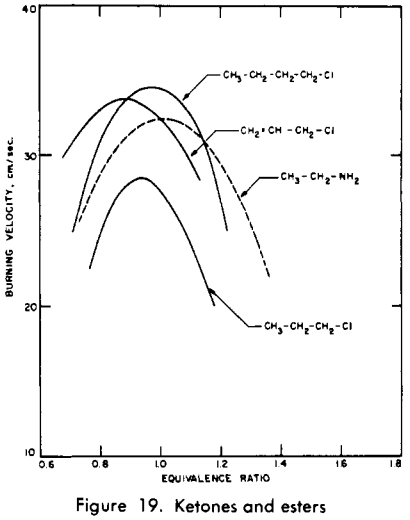

Figure 19. Ketones and esters

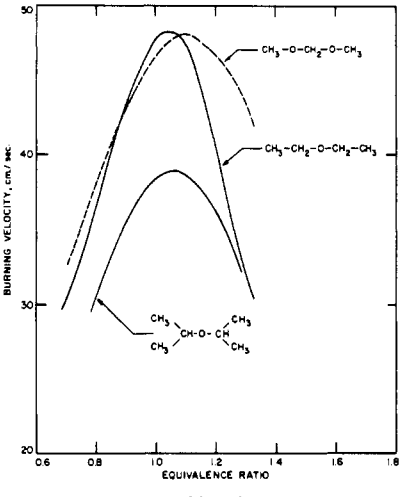

Figure 20. Ethers

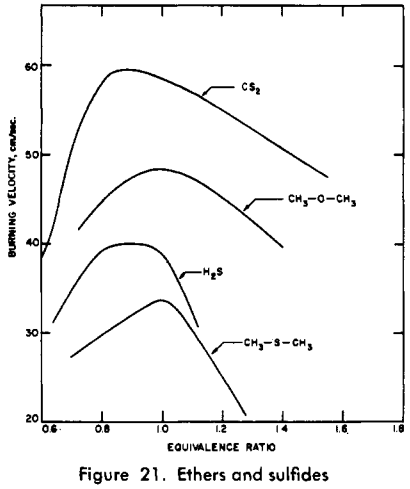

Figure 21. Ethers and sulfides

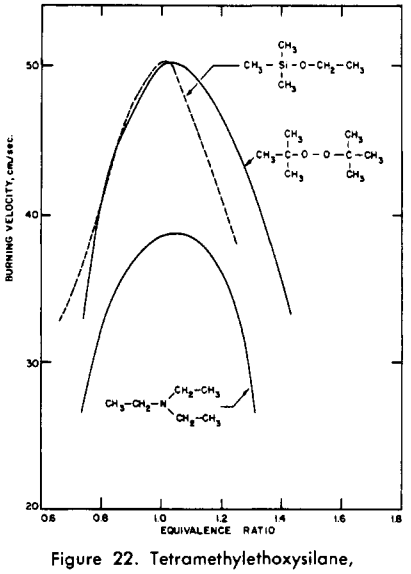

Figure 22. Tetramethylethoxysilane, di-*tert*-butyl peroxide, and triethylamine

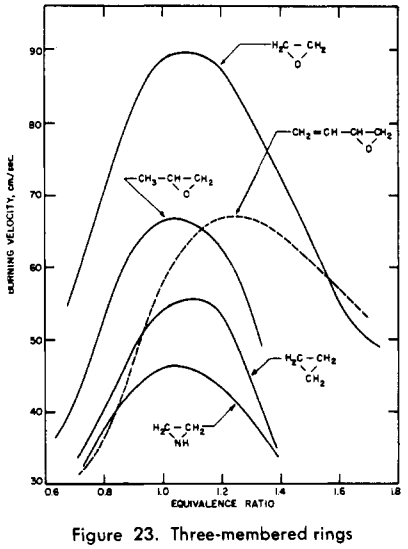

Figure 23. Three-membered rings

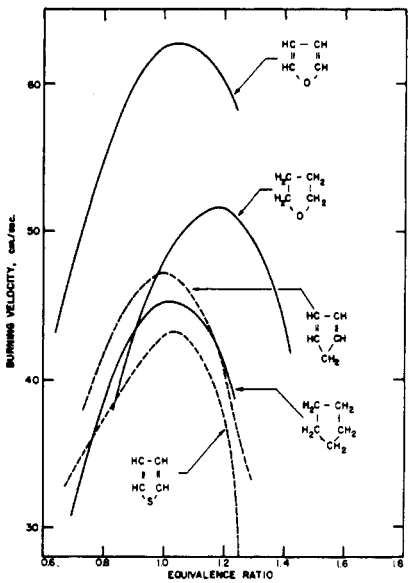

Figure 24. Five-membered rings

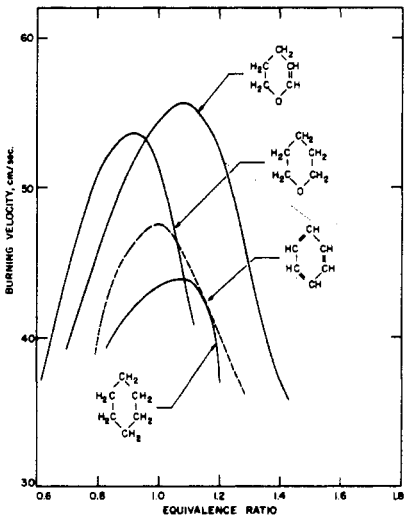

Figure 25. Six-membered rings

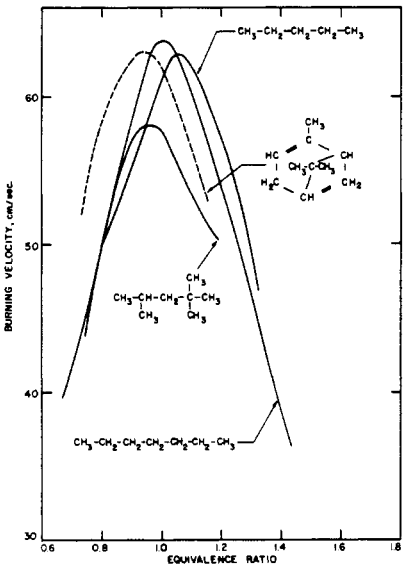

Figure 26. Hydrocarbons

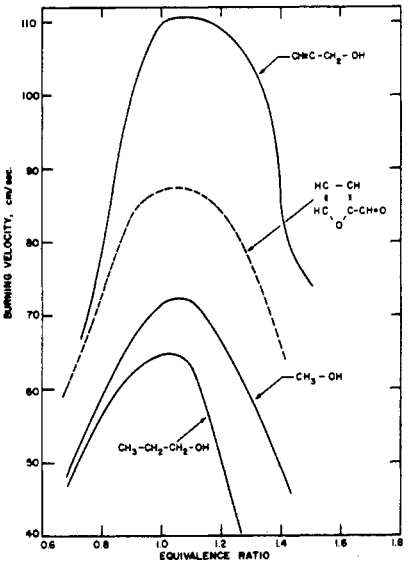

Figure 27. Alcohols and furfural

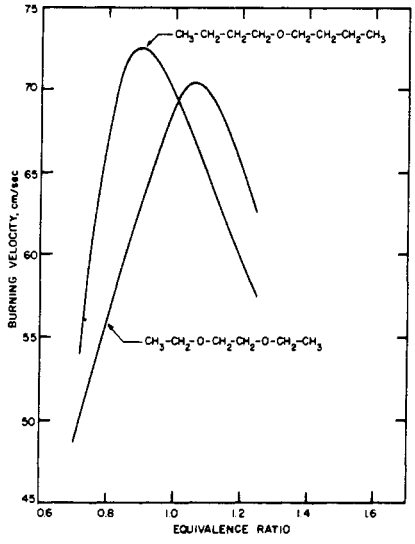

Figure 28. *n*-Butyl ether and diethyl Cellosolve

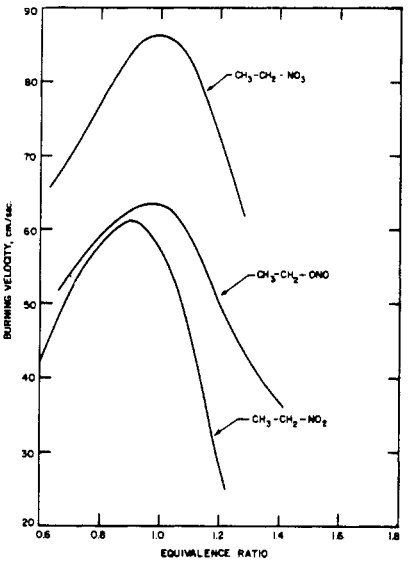

Figure 29. Ethyl nitrate, ethyl nitrite, and nitroethane

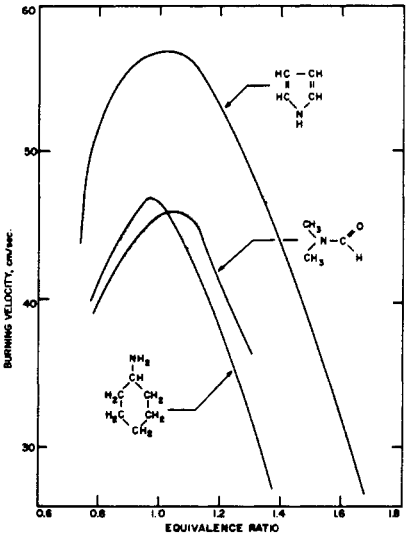

Figure 30. Pyrrole, dimethylformamide, and aniline

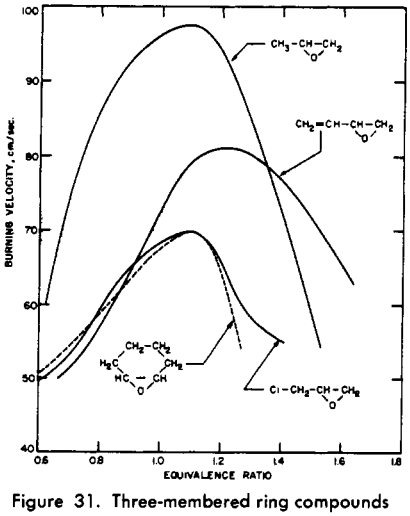

Figure 31. Three-membered ring compounds

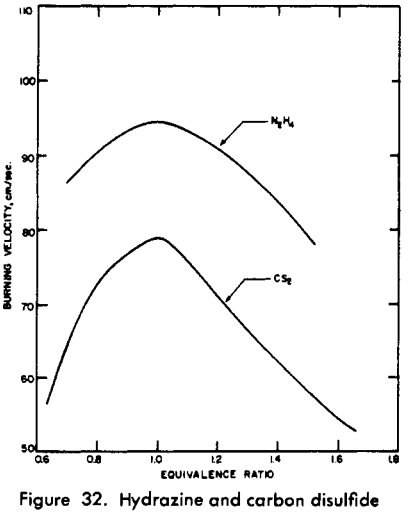

Figure 32. Hydrazine and carbon disulfide

Effect of Molecular Structure
on Burning Velocities, 25° C.

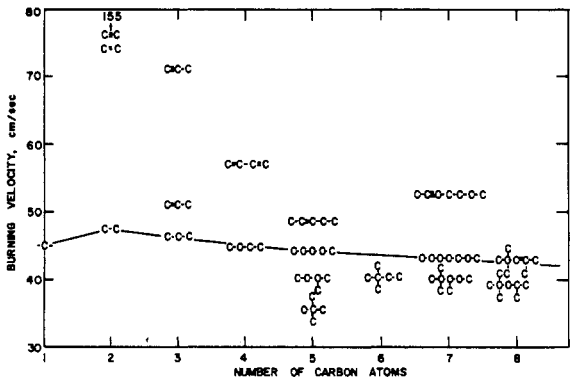

Figure 33.
Hydrocarbons

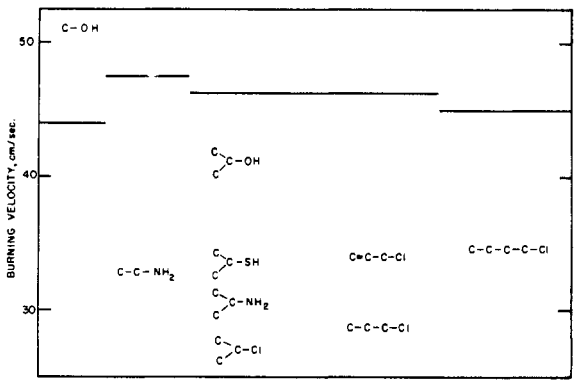

Figure 34.
Substituted
hydrocarbons

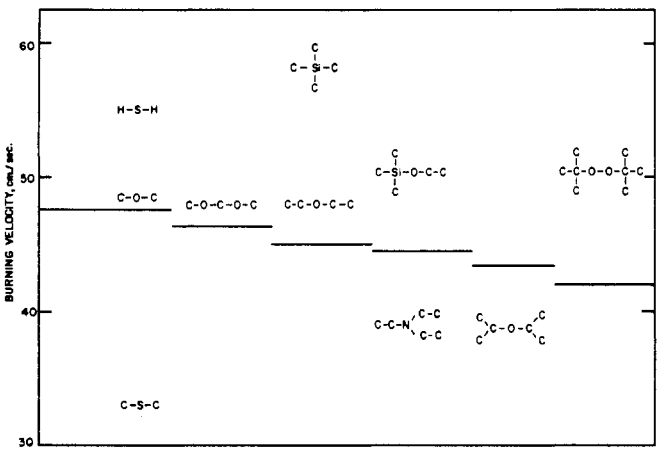

Figure 35. Compounds containing oxygen, sulfur, nitrogen, or silicon

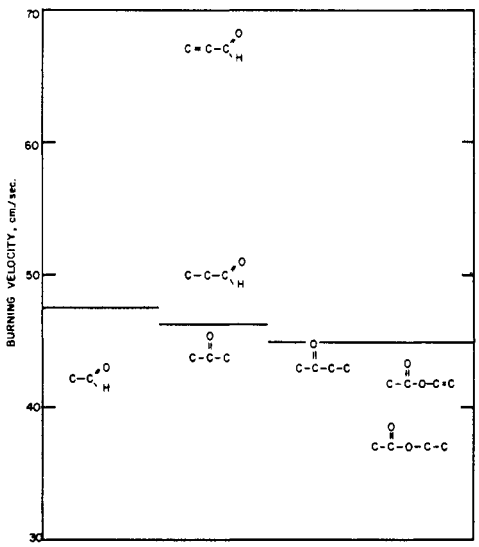

Figure 36. Aldehydes, ketones, and esters

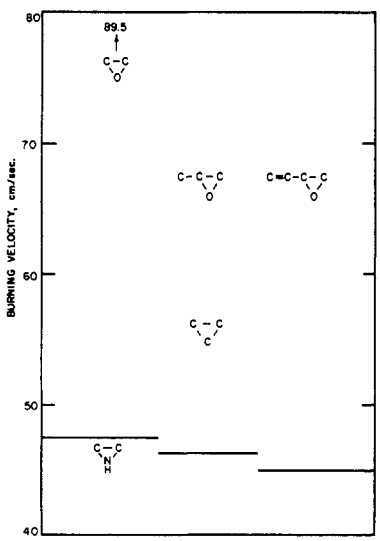

Figure 37. Three-membered ring compounds

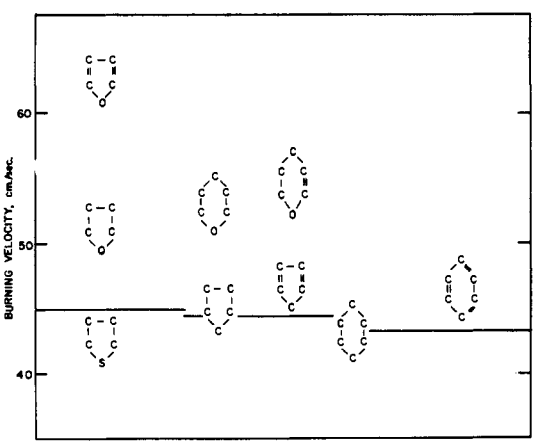

Figure 38. Five- and six-membered rings

Appearance of flames. Aniline. The inner cone was blue with a reddish yellow outer cone. At $\phi = 1$ a yellow tip appeared at the apex of the inner cone and became larger for richer mixtures.

Ethylamine. A yellow tip appeared at approximately $\phi = 1.25$.

Pyrrole. At $\phi = 1.25$ a yellow tip appeared on the apex of the inner cone. At $\phi = 1.35$ three distinct cones appeared; from inner to outer these were blue, dark blue, and greenish blue with a yellow tip on the inner cone.

Thiophene. The inner cone was blue with a deep purple outer cone which increased in intensity for richer mixtures. At $\phi = 1.25$ multiple cones began to appear; from inner to outer, these were blue, white, purple, and blue white with a yellow tip just above the inner cone.

The effect of molecular structure on the maximum velocity is presented graphically in Figures 33 to 40. The maximum burning velocity in centimeters per second is recorded on the ordinate, and the abscissa indicates structural changes and generally the number of carbon atoms in the molecule. On each figure a horizontal line has been drawn to indicate the burning velocity of the normal alkane hydrocarbon.

Hydrocarbon burning velocities fall in order: alkynes > alkenes > alkanes. Conjugation generally increases the burning velocity; chain lengthening and branching decrease the burning velocity, but structural alterations become less effective as the chain length is increased (Figure 33).

Negative substituent groups decrease the burning velocity. In order of increasing effectiveness they are alcohol, mercaptan, amine, and chloride, which is about equal to the epoxy group, and is more effective than a double bond—*i.e.*, allyl chloride burns considerably slower than propylene, but only slightly slower than *n*-butyl chloride because the effect of molecular alterations becomes less important as the chain length is increased (Figure 34).

Silicon in the molecule increases the burning velocity (Figure 35). The sulfide group (Figures 35 and 38) and nitrogen (Figures 34, 35, 37, and 39) generally decrease it, excepting in ethyl nitrate (Figure 40).

Peroxide, aldehyde, and ether groups (especially in cyclics) have high burning velocities, but ketones and esters have somewhat lower burning velocities than the parent hydrocarbon (Figures 36, 38, and 40).

Three-membered ring compounds except ethylenimine, which contains nitrogen, have higher burning velocities than the corresponding alkane, the oxygen-containing ring being particularly effective (Figure 37). Five- and six-membered rings as well as aromatic structures have little effect on the burning velocity relative to the linear hydrocarbon containing the same number of carbon atoms. (Figure 38).

Compounds with insufficient vapor pressure to be studied at 25° C were examined at 100° C with enough repeats to make comparisons (Figures 39 and 40). The results are consistent with observations made at 25° C. Pinene shows no change in burning velocity from the alkane containing the same number of carbon atoms.

To predict the burning velocity of any specific substance, a comparison of its structure with these examples should be fruitful. However, before any more detailed analysis of the molecular structure effects can be made profitably, the thermodynamic, energy and mass transport, and chemical-kinetic properties of the systems involved must be considered. Such an analysis should help in unraveling the intricate relationship between the above-mentioned principles and make available a better understanding of the mechanism of flame propagation.

ACKNOWLEDGMENT

The authors acknowledge the contributions of the following, who at one time or another participated in this program: W. G. Atkins, C. B. Barnett, R. B. Huettel, M. R. Irby, and A. R. Sharpe, Jr.

LITERATURE CITED

(1) Andersen, J. W., Fein, R. S., *J. Chem. Phys.* **17,** 1268-73 (1949); **18,** 441-3 (1950).
(2) Ashforth, G. K., *Fuel* **29,** 284-7 (1950).
(3) Badin, E. J., Stuart, J. G., Pease, R. N., *J. Chem. Phys.* **17,** 314-6 (1949).
(4) Bartholomé, E., *Z. Elektrochem.* **53,** 191-6 (1949); *Naturwissen schaften* **36,** 171-5, 206-13 (1949).
(5) Calcote, H. F., *Anal. Chem.* **22,** 1058-60 (1950).
(6) Calcote, H. F., Gregory, C. A., Jr., Barnett, C. M., Gilmer, R. B., *Ind. Eng. Chem.* **44,** 2656-62 (1952).
(7) Caldwell, F. R., Broida, H. P., Dover, J. J., *Ibid.*, **43,** 2731-9 (1951).
(8) Clingman, W. H., Brokaw, R. S., Pease, R. N., "Fourth Symposium (International) on Combustion," pp. 310-13, Williams & Wilkins Co., Baltimore, 1953.
(9) Conan, H. R., Linnett, J. W., *Trans. Faraday Soc.* **47,** 981-8 (1951).
(10) Dugger, G. L., *J. Am. Chem. Soc.* **72,** 5271-4 (1950).
(11) Fenn, J. B., Calcote, H. F., "Fourth Symposium (International) on Combustion," pp. 231-9, Williams & Wilkins Co., Baltimore, 1953.
(12) Fiock, E. F., "Physical Measurements in Gas Dynamics and Combustion," Part 2, pp. 409-38, Princeton University Press, Princeton, N. J., 1954.
(13) Friedman, R., Burke, E., *Ind. Eng. Chem.* **43,** 2772-6 (1951).
(14) Garner, F. H., Long, R., Ashforth, G. K., *Fuel* **28,** 272-6 (1949); **30,** 17-19 (1951).
(15) Garner, F. H., Long, R., Thorley, B., "Fourth Symposium (International) on Combustion," pp. 386-92, Williams & Wilkins Co., Baltimore, 1953.

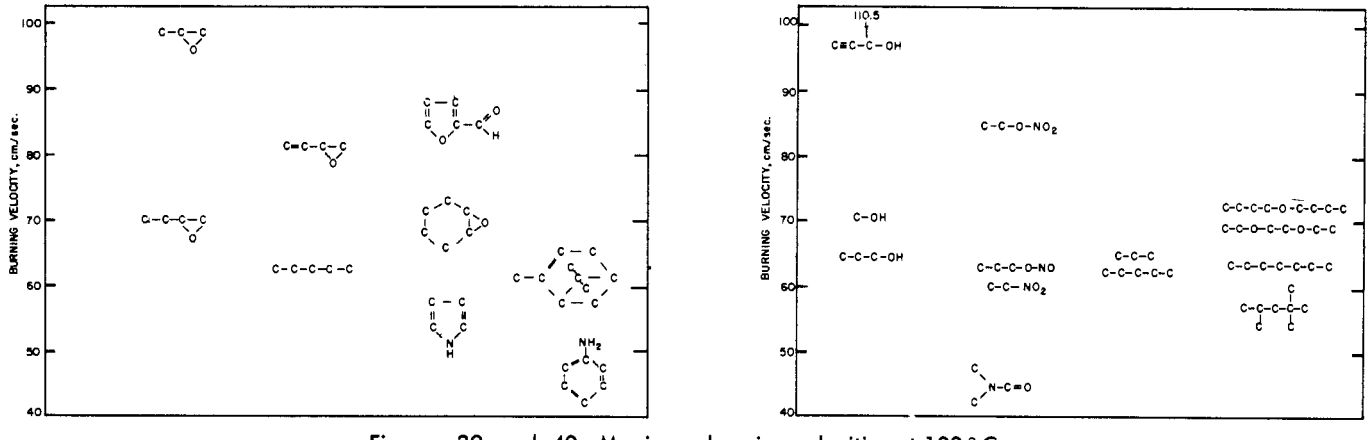

Figures 39 and 40. Maximum burning velocities at 100° C.

Table V. Burning Velocities of Various Fuels at 25° C. Air-Fuel Temperature

(0.31 mole-% H_2O in air)

	Burning velocity, S, as a function of equivalence ratio, ϕ, in cm./sec.									
	ϕ = 0.7	0.8	0.9	1.0	1.1	1.2	1.3	1.4	$S_{max.}$	ϕ at $S_{max.}$
Saturated hydrocarbons										
Ethane	30.6	36.0	40.6	44.5	47.3	47.3	44.4	37.4	47.6	1.14
Propane			42.3	45.6	46.2	42.4	34.3		46.4	1.06
n-Butane		38.0	42.6	44.8	44.2	41.2	34.4	25.0	44.9	1.03
Methane		30.0	38.3	43.4	44.7	39.8	31.2		44.8	1.08
n-Pentane		35.0	40.5	42.7	42.7	39.3	33.9		43.	1.05
n-Heptane		37.0	39.8	42.2	42.0	35.5	29.4		42.8	1.05
2, 2, 4-Trimethylpentane		37.5	40.2	41.0	37.2	31.0	23.5		41.0	0.98
2, 2, 3-Trimethylpentane		37.8	39.5	40.1	39.5	36.2			40.1	1.00
2, 2-Dimethylbutane		33.5	38.3	39.9	37.0	33.5			40.0	0.98
Isopentane		33.0	37.6	39.8	38.4	33.4	24.8		39.9	1.01
2, 2-Dimethylpropane			31.0	34.8	36.0	35.2	33.5	31.2	36.0	1.10
Unsaturated hydrocarbons										
Acetylene		107	130	144	151	154	154	152	155	1.25
Ethylene	37.0	50.0	60.0	68.0	73.0	72.0	66.5	60.0	73.5	1.13
Propyne		62.0	66.6	70.2	72.2	71.2	61.0		72.5	1.14
1, 3-Butadiene			42.6	49.6	55.0	57.0	56.9	55.4	57.2	1.23
n-1-Heptyne		46.8	50.7	52.3	50.9	47.4	41.6		52.3	1.00
Propylene			48.4	51.2	49.9	46.4	40.8		51.2	1.00
n-2-Pentene		35.1	42.6	47.8	46.9	42.6	34.9		48.0	1.03
2, 2, 4-Trimethyl-3-pentene		34.6	41.3	42.2	37.4	33.0			42.5	0.98
Substituted alkyls										
Methanol		34.5	42.0	48.0	50.2	47.5	44.4	42.2	50.4	1.08
Isopropyl alcohol		34.4	39.2	41.3	40.6	38.2	36.0	34.2	41.4	1.04
Triethylamine		32.5	36.7	38.5	38.7	36.2	28.6		38.8	1.06
n-Butyl chloride	24.0	30.7	33.8	34.5	32.5	26.9	20.0		34.5	1.00
Allyl chloride	30.6	33.0	33.7	32.4	29.6				33.8	0.89
Isopropyl mercaptan		30.0	33.5	33.0	26.6				33.8	0.94
Ethylamine		28.7	31.4	32.4	31.8	29.4	25.3		32.4	1.00
Isopropylamine		27.0	29.5	30.6	29.8	27.7			30.6	1.01
n-Propyl chloride		24.7	28.3	27.5	24.1				28.5	0.93
Isopropyl chloride		24.8	27.0	27.4	25.3				27.6	0.97
n-Propyl bromide	No ignition									
Silanes										
Tetramethylsilane	39.5	49.5	57.3	58.2	57.7	54.5	47.5		58.2	1.01
Trimethylethoxysilane	34.7	41.0	47.4	50.3	46.5	41.0	35.0		50.3	1.00
Aldehydes										
Acrolein	47.0	58.0	66.6	65.9	56.5				67.2	0.95
Propionaldehyde		37.5	44.3	49.0	49.5	46.0	41.6	37.2	50.0	1.06
Acetaldehyde		26.6	35.0	41.4	41.4	36.0	30.0		42.2	1.05
Ketones										
Acetone		40.4	44.2	42.6	38.2				44.4	0.93
Methyl ethyl ketone		36.0	42.0	43.3	41.5	37.7	33.2		43.4	0.99
Esters										
Vinyl acetate	29.0	36.6	39.8	41.4	42.1	41.6	35.2		42.2	1.13
Ethyl acetate		30.7	35.2	37.0	35.6	30.0			37.0	1.00
Ethers										
Dimethyl ether		44.8	47.6	48.4	47.5	45.4	42.6		48.6	0.99
Diethyl ether	30.6	37.0	43.4	48.0	47.6	40.4	32.0		48.2	1.05
Dimethoxymethane	32.5	38.2	43.2	46.6	48.0	46.6	43.3		48.0	1.10
Diisopropyl ether		30.7	35.5	38.3	38.6	36.0	31.2		38.9	1.06
Thio ethers										
Dimethyl sulfide		29.9	31.9	33.0	30.1	24.8			33.0	1.00
Peroxides										
Di-*tert*-butyl peroxide		41.0	46.8	50.0	49.6	46.5	42.0	35.5	50.4	1.04
Aromatic compounds										
Furan	48.0	55.0	60.0	62.5	62.4	60.0			62.9	1.05
Benzene		39.4	45.6	47.6	44.8	40.2	35.6		47.6	1.00
Thiophene	33.8	37.4	40.6	43.0	42.2	37.2	24.6		43.2	1.03
Cyclic compounds										
Ethylene oxide	57.2	70.7	83.0	88.8	89.5	87.2	81.0	73.0	89.5	1.07
Butadiene monoxide		36.6	47.4	57.8	64.0	66.9	66.8	64.5	67.1	1.24
Propylene oxide	41.6	53.3	62.6	66.5	66.4	62.5	53.8		67.0	1.05
Dihydropyran	39.0	45.7	51.0	54.5	55.6	52.6	44.3	32.0	55.7	1.08
Cyclopropane		40.6	49.0	54.2	55.6	53.5	44.0		55.6	1.10
Tetrahydropyran	44.8	51.0	53.6	51.5	42.3				53.7	0.93

Table V. Continued

(0.31 mole-% H_2O in air)

Burning velocity, S, as a function of equivalence ratio, ϕ, in cm./sec.

	ϕ = 0.7	0.8	0.9	1.0	1.1	1.2	1.3	1.4	$S_{max.}$	ϕ at $S_{max.}$
Cyclic compounds										
Tetrahydrofuran			43.2	48.0	50.8	51.6	49.2	44.0	51.6	1.19
Cyclopentadiene	36.0	41.8	45.7	47.2	45.5	40.6	32.0		47.2	1.00
Ethylenimine		37.6	43.4	46.0	45.8	43.4	38.9		46.4	1.04
Cyclopentane	31.0	38.4	43.2	45.3	44.6	41.0	34.0		45.4	1.03
Cyclohexane			41.3	43.5	43.9	38.0			44.0	1.08
Inorganic compounds										
Hydrogen	102	120	145	170	204	245	213	290	325	1.80
Carbon disulfide	50.6	58.0	59.4	58.8	57.0	55.0	52.8	51.6	59.4	0.91
Carbon monoxide					28.5	32.0	34.8	38.0	52.0	2.05
Hydrogen sulfide	34.8	39.2	40.9	39.1	32.3				40.9	0.90

Table VI. Burning Velocities of Various Fuels at 100° C. Air-Fuel Temperature

(0.31 mole-% H_2O in Air)

Burning velocity, S, as a function of equivalence ratio, ϕ in cm./sec.

	ϕ = 0.7	0.8	0.9	1.0	1.1	1.2	1.3	1.4	$S_{max.}$	ϕ at $S_{max.}$
Propargyl alcohol		76.8	100.0	110.0	110.5	108.8	105.0	85.0	110.5	1.08
Propylene oxide	74.0	86.2	93.0	96.6	97.8	94.0	84.0	71.5	97.9	1.09
Hydrazine[a]	87.3	90.5	93.2	94.3	93.0	90.7	87.4	83.7	94.4	0.98
Furfural	62.0	73.0	83.3	87.0	87.0	84.0	77.0	65.5	87.3	1.05
Ethyl nitrate	70.2	77.3	84.0	86.4	83.0	72.3			86.4	1.00
Butadiene monoxide	51.4	57.0	64.5	73.0	79.3	81.0	80.4	76.7	81.1	1.23
Carbon disulfide	64.0	72.5	76.8	78.4	75.5	71.0	66.0	62.2	78.4	1.00
n-Butyl ether		67.0	72.6	70.3	65.0				72.7	0.91
Methanol	50.0	58.5	66.9	71.2	72.0	66.4	58.0	48.8	72.2	1.08
Diethyl cellosolve	49.5	56.0	63.0	69.0	69.7	65.2			70.4	1.05
Cyclohexene monoxide	54.5	59.0	63.5	67.7	70.0	64.0			70.0	1.10
Epichlorohydrin	53.0	59.5	65.0	68.6	70.0	66.0	58.2		70.0	1.10
n-Pentane		50.0	55.0	61.0	62.0	57.0	49.3	42.4	62.9	1.05
n-Propyl alcohol	49.0	56.6	62.0	64.6	63.0	50.0	37.4		64.8	1.03
n-Heptane	41.5	50.0	58.5	63.8	59.5	53.8	46.2	38.8	63.8	1.00
Ethyl nitrite	54.0	58.8	62.6	63.5	59.0	49.5	42.0	36.7	63.5	1.00
Pinene	48.5	58.3	62.5	62.1	56.6	50.0			63.0	0.95
Nitroethane	51.5	57.8	61.4	57.2	46.0	28.0			61.4	0.92
Iso-octane		50.2	56.8	57.8	53.3	50.5			58.2	0.98
Pyrrole		52.0	55.6	56.6	56.1	52.8	48.0	43.1	56.7	1.00
Aniline		41.5	45.4	46.6	42.9	37.7	32.0		46.8	0.98
Dimethyl formamide		40.0	43.6	45.8	45.5	40.7	36.7		46.1	1.04

[a]Results questionable because of an indication of decomposition in the stainless-steel feed system.

(16) Garside, J. E., Forsyth, J. S., Townend, D. T. A., *J. Inst. Fuel* **18,** 175 (1945).
(17) Gaydon, A. G., Wolfhard, H. G., "Flames, Their Structure, Radiation and Temperature," Chapman and Hall, London, 1953.
(18) Gerstein, M., Levine, O., Wong, E. L., *J. Am. Chem. Soc.* **73,** 418–22 (1951); *Ind. Eng. Chem.* **43,** 2770–2 (1951).
(19) Gouy, M., *Ann. chim. phys.* **18,** 27 (1879).
(20) Gray, K. L., Linnett, J. W., Mellish, C. E., *Trans. Faraday Soc.* **48,** 1155–63 (1952).
(21) Grove, J. R., Hoare, M. F., Linnett, J. W., *Ibid.*, **46,** 745–55 (1950).
(22) Jost, Wilhelm, "Explosion and Combustion Processes in Gases," trans. by H. O. Croft, McGraw-Hill, New York, 1946.
(23) Kapp, N. M., Snow, B., Wohl, K., "Effect of Water Vapor on the Normal Burning Velocity and on the Stability of Butane-Air Flames Burning above Tubes in Free Air," United Aircraft Corp. Meteor Rep. **UAC-30** (Nov. 1948).
(24) Levine, O., Gerstein, M., "Fundamental Flame Velocities of Pure Hydrocarbons, III," NACA Research Mem. **RM E51J05** (Dec. 3, 1951).
(25) Lewis, B., von Elbe, G., *J. Chem. Phys.* **11,** 75 (1943); "Combustion, Flames and Explosions of Gases," Academic Press, New York, 1951.
(26) Linnett, J. W., Hoare, M. F., *Trans. Faraday Soc.* **47,** 179–83 (1951); **49,** 1038–49 (1953).
(27) Linnett, J. W., Pickering, H. S., Wheatley, P. J., *Ibid.*, **47,** 974–80 (1951).
(28) Manton, J., von Elbe, G., Lewis, B., "Fourth Symposium (International) on Combustion," pp. 358–63, Williams & Wilkins Co., Baltimore, 1953.
(29) Pickering, H. S., Linnett, J. W., *Trans. Faraday Soc.* **47,** 989–92 (1951); **47,** 1101–06 (1951).
(30) Reynolds, T. W., Gerstein, M., "Third Symposium on Combustion and Flame and Explosion Phenomena," pp. 190-4, Williams & Wilkins Co., Baltimore, 1949.
(31) Sherratt, S., Linnett, J. W., *Trans. Faraday Soc.* **44,** 596–608 (1948).
(32) Simon, D. M., *Ind. Eng. Chem.* **43,** 2718–21 (1951).
(33) Singer, J. M., "Fourth Symposium (International) on Combustion," pp. 352–358, Williams & Wilkins Co., Baltimore, 1953.
(34) Smith, F. A., Pickering, S. F., *J. Research Natl. Bur. Standards* **17,** 7–43 (1936).
(35) Strehlow, R. A., Stuart, J. G., "Fourth Symposium (International) on Combustion," pp. 329–36, Williams & Wilkins Co., Baltimore, 1953.
(36) Wheatley, P. J., Linnett, J. W., *Trans. Faraday Soc.* **48,** 338–45 (1952).

RECEIVED for review January 21, 1958. Accepted October 8, 1958. This work was carried out for the Department of the Navy, Bureau of Ordnance, under contract NOrd-9756, as part of Project Bumblebee.